ELSEVIER

Journal of Power Sources 96 (2001) 343–351

JOURNAL OF POWER SOURCES

www.elsevier.com/locate/jpowsour

Simulation and analysis of time-dependent degradation behavior of AMTEC

M.A.K. Lodhi[a,*], P. Vijayaraghavan[b], A. Daloglu[a,1]

[a]*Department of Physics, Texas Technical University, Box 41051, Lubbock, TX 79409-1051, USA*
[b]*Department of Mechanical Engineering, Texas Technical University, Box 41051, Lubbock, TX 79409-1051, USA*

Received 20 October 2000; accepted 7 November 2000

Abstract

Alkali metal thermal-to-electric converter (AMTEC) technology is ideally suited for a wide range of applications from space, aerospace and military to domestic and other terrestrial civilian applications.

In spite of its many advantages, existing AMTEC technology has some drawbacks that prevent the realization of the full potential of the technology. The problem is that the cell efficiency is still below its theoretically achievable value, and the cell has an adverse power-time characteristic. The maximum power output of the cell was observed to decrease from 2.54 W at the end of 172 h to 1.27 W during its 18,000 h of cell operation. This problem may preclude the use of the cell for applications that require operation of the cell for long periods of time.

This paper deals with the factors responsible for this degradation and discusses in detail the simulation model used to study and predict the performance of the cell as a function of time. It is shown that the β-alumina solid electrolyte is a major cause of this degradation and a model to simulate its performance is developed and compared with available experimental data to establish the role of the electrolyte.

Keywords: AMTEC; Power degradation; Ionic resistance; Solid electrolytes; Space power; Efficiency

1. Introduction

Alkali metal thermal-to-electric converters (AMTECs) belong to the class of static converters that produce electricity directly from heat energy, the other class being dynamic converters. As the names suggest, dynamic converters rely essentially on the movement of parts for the energy conversion process while static converters do not involve any moving parts in the generation of electricity. Dynamic converters remain the mainstay of large-scale electric generation. However, static converters are finding newer applications and their importance has been on the rise in recent times.

The AMTEC is a thermally regenerative, electrochemical device. Thermal regeneration means that the heat of the working fluid is not removed from the system at the end of a working cycle as is done in an internal combustion engine where some of the heat supplied to the fuel is released outside the system through the exhaust gases. The heat of the working fluid is instead re-used in the next cycle (actually, the fluid itself is re-circulated) thereby increasing efficiency. This system uses an alkali metal (lithium, sodium or potassium) in its process. The electrochemical process involved is the ionization of the alkali metal atoms at the interface of the electrode and the electrolyte. The electrons produced as a result flow through the external load, thus, doing work and finally re-combine with the ions to form neutral atoms at the other electrode (cathode). Alkali metal thermal-to-electric converters offer many advantages over conventional forms of electricity production. While some of these are common to static converters in general, others are almost uniquely associated with AMTEC technology. Some of the advantages are listed below.

1. High efficiency: this is one of the most important advantages. Alkali metal thermal-to-electric converters have very high efficiencies and can theoretically perform close to Carnot efficiency. Optimized AMTEC designs can work up to 40% efficiency at hot-side temperatures of about 1000–1300 K and cold-end temperatures of 400–700 K [1–3].

* Corresponding author. Tel.: +1-806-742-3778; fax: +1-806-742-1182.
E-mail address: b5mak@ttacs.ttu.edu (M.A.K. Lodhi).
[1] Present address. Department of Mechanical Engineering, Karadeniz Technical University, 61081 Trabzon, Turkey.

0378-7753/01/$ – see front matter © 2001 Published by Elsevier Science B.V.
PII: S0378-7753(00)00664-9

2. High power density: alkali metal thermal-to-electric converters have high power densities. With some designs, the calculated density of 19.8 W/kg has been obtained and this value can go up to 0.5 kW/kg in optimized design [4].
3. Absence of moving parts ensures that problems of lubrication, wear and tear and noise are eliminated, and makes AMTECs virtually maintenance-free devices requiring very little or no external intervention once the system starts functioning.
4. Alkali metal thermal-to-electric converters are extremely reliable because of the absence of chemical reactions and that of moving parts.
5. Though AMTECs are high-performance devices, the materials used in the construction are easily available and the fabrication of the cell itself can be achieved at very economical costs.
6. The working temperatures of AMTECs allow cascading of the cell with other electric-generation devices in which the heat-rejecting side of the other device is thermally connected to the hot side of the AMTEC resulting in efficiencies higher than the individual efficiency of either system [5–7].
7. Alkali metal thermal-to-electric converters typically generate high-current, low-voltage electrical output. AMTEC cells are amenable to modular design. This means that large-scale power systems can be built by electrically connecting smaller cells together [8,9].

In spite of the aforementioned advantages of AMTEC technology, the current designs suffer with some problems. One of these is the failure to achieve optimal efficiency. Efficiencies in the range of 10–15% only have been attained so far. This can be attributed to design factors. A more serious problem is that of a steady reduction in power output of the cell with time. In case of the PX-3A model of AMTEC, the power output drops rapidly. The maximum power output, 2.45 W, measured at the end of 172 h dropped to 1.27 W during its 18,000 h testing period since July 1997 at Air Force Research Laboratory (AFRL), Albuquerque, NM. This drop in power output also means that efficiency of the cell reduces accordingly. This problem will prevent the cell from being used in applications that require a certain minimum power supply over a long period of time. Typical applications with such requirements include deep-space exploration and remote site applications.

In this paper, we are looking from an extended computer simulation study, the factors responsible for power degradation of AMTEC when operated for a long period of time. For that we briefly examine the working principle of AMTEC and the role of its important components and prepare an empirical model.

2. Working of the AMTEC and the role of the BASE in power degradation

The working of the PX-3A AMTEC cell is shown schematically in Fig. 1. The most important component of the AMTEC is the electrolyte. Unlike many other fuel cells, AMTEC uses a ceramic solid electrolyte of β-alumina. This material has a unique property that it allows only cations to

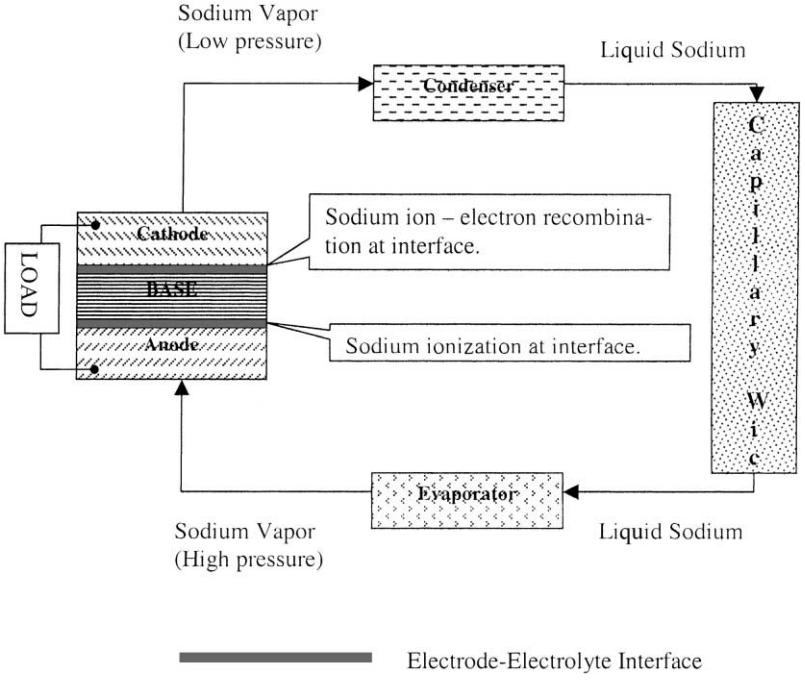

Fig. 1. Schematic diagram of the vapor-fed AMTEC cycle.

pass through it while it is impermeable to neutral or negatively charged particles including electrons. It is this property that is used in the AMTEC to produce electric current. The working fluid in AMTECs is an alkali metal in either the liquid or vapor state or both. In the PX-3A model AMTEC, the β-alumina solid electrolyte (BASE) is in contact with high-pressure sodium vapor on one side and with low-pressure sodium vapor on the other. Electrodes are deposited on these two sides of the BASE to provide electrical contact. Sodium vapor on the high-pressure side tries to expand as a result of the pressure differential with respect to the low-pressure side but is constrained by the solid electrolyte. The only way the pressure energy can be released is for the sodium atoms to ionize and the ions to then pass through the BASE. The atoms, therefore, ionize at the interface between the anode and the BASE. While the positive ions flow through the BASE material, the electrons flow from the anode, through the external electrical load, to the cathode where they recombine with the ions that have passed through the BASE to form neutral sodium atoms. The flow of electrons through the external load is what produces the electrical power. The recombination of sodium ions and electrons gives rise to low-pressure sodium vapor which is condensed at the condenser and circulated to the evaporator by means of a capillary liquid return artery. The evaporator converts this liquid sodium to high-pressure sodium vapor and this cycle is repeated for the continuous production of electricity [10–12].

The BASE is one of the most important components of the AMTEC. It is on the unique conduction property of β-alumina that the working of the AMTEC is based. Any change in the properties of the BASE can significantly affect power generation. In fact, the BASE does undergo several changes in its material and conduction properties during the AMTEC operation. These changes can be broadly classified as thermal breakdown and chemical contamination [13,14]. Thermal breakdown is in the form of loss of sodium from the material, formation of molten dendrites in the material, crack formation and propagation, and changes in the microstructure. Loss of sodium from the BASE can increase its ionic resistance [15]. Molten dendrites propagate through the thickness of the BASE tube and can give rise to an electrical short between the cathode and the anode reducing electron flow through the external load [16]. When cracks propagate through the thickness of the BASE tube, they can cause some sodium vapor to flow from the high-pressure to the low-pressure side without the sodium atoms having ionized [16]. This again will cause fewer electrons to be available for flow through the external load. Changes in the microstructure like grain growth will increase the ionic resistance of the BASE. Chemical contamination is the result of chemical reactions between the high-pressure, high-temperature sodium vapor and the stainless steel used in many of the components of the cell. The products of these reactions will enter the sodium stream, and either deposit on the surface of the BASE, thus, blocking the pores or enter the crystal structure of the BASE in which case they may either deposit on the grain boundary or replace some ions in the structure [17–21]. In all these three cases, the effect is an increase in the ionic resistance of the BASE. Thus, changes in the BASE affect adversely the power output of the cell.

3. Modeling of BASE resistance

These changes occur over a period of time, sometimes over thousands of hours of cell operation. The effect of these changes on power output is the same as an increase in the ionic resistance alone of the BASE. Therefore, changes in the properties of the BASE are modeled as a change in the ionic resistance as a function of time in order to simulate the time-dependent power output of the cell as a whole. In this work, attention is only focused on the change in BASE ionic resistance. This does not, however, imply that other components do not undergo any change. As a first step, an expression for BASE resistance with time is determined to generate a power versus time characteristic similar to the observed power degradation. This modeling is performed using a FORTRAN code to simulate the steady-state performance of the PX-3A called the AMTEC performance and evaluation analysis model (APEAM). In order to do this, it is necessary to vary BASE resistance with respect to time. However, the BASE resistance is defined not as a single value but as an array in the simulation program. The APEAM discretises the BASE tube into several cells within each of which the temperature and resistance are assumed to remain constant for purposes of analysis. Moreover, the array for BASE resistance is evaluated as an expression. Therefore, to study the effect of BASE resistance it is not possible to use absolute values for BASE resistance in the existing APEAM program. This problem can be circumvented by multiplying the expression for BASE resistance with some positive real number. This has the same effect as varying the BASE resistance in multiples.

4. Regression analysis

Having devised a method to vary BASE resistance, the next step is to determine an expression for changing BASE resistance with time that will generate a power versus time characteristic similar to the observed power degradation. The procedure adopted is as follows. The data for power degradation starts at 172 h with 2.45 W power output. At the beginning, unity is used as the multiple for the expression of the BASE resistance which corresponds to the initial value of BASE resistance, and to the first reading in the data, namely, 172 h and 2.45 W. Thereafter, the multiple is increased in either decimal or whole number steps. For each reading of the experimental data for power degradation, that multiple to the expression of the BASE resistance is

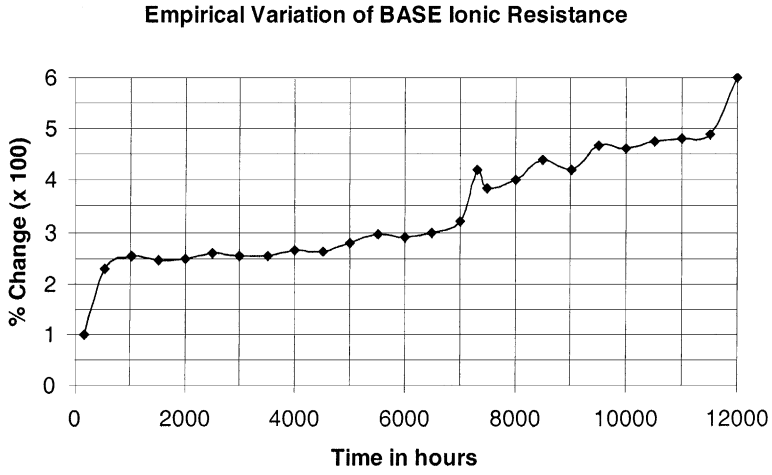

Fig. 2. Empirical variation of the ionic resistance of the BASE that gives the observed power degradation.

determined such that it gives the experimentally observed power output at that reading (point of time). That value of resistance is, then, what the BASE attains at that time. This procedure is repeated for each reading in the data. Thus, a set of data is obtained that shows the value of BASE resistance at each point of time given on the data for power degradation. At that point, it is remembered that the procedure described above has two aspects to it: (1) it approximates all the changes in the BASE as an increase in its ionic resistance and (2) it models the BASE resistance as representative of all the changes in the AMTEC because the properties of other components in the cell are assumed constant with time. Thus, the BASE resistance simulates the cumulative effect of properties of all the components in the cell, and any change in BASE resistance values reflects the overall change for all the AMTEC components. The variation of BASE resistance with time obtained is shown in Fig. 2 which in fact represents the change in total internal resistance of the cell and, thus, the effect of all the components and materials in the cell. To test the validity of this variation in the ionic resistance of the BASE, a regression analysis is first performed on the variation to obtain suitable equations to describe it. The analysis is performed using the plotting and statistical package XMGR on a Linux platform. We tried three functions, namely, exponential, power and logarithmic to obtain the matching whose fits are shown in Fig. 3. The

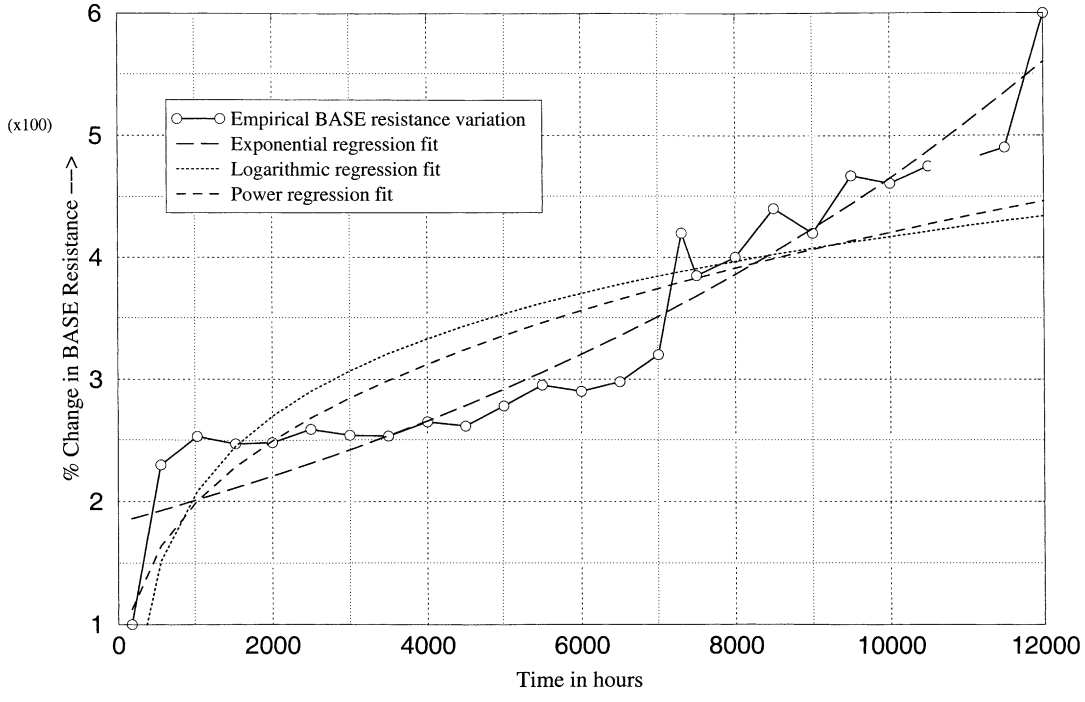

Fig. 3. Exponential, logarithmic and power regrerssion fits for empirical BASE resistance variation.

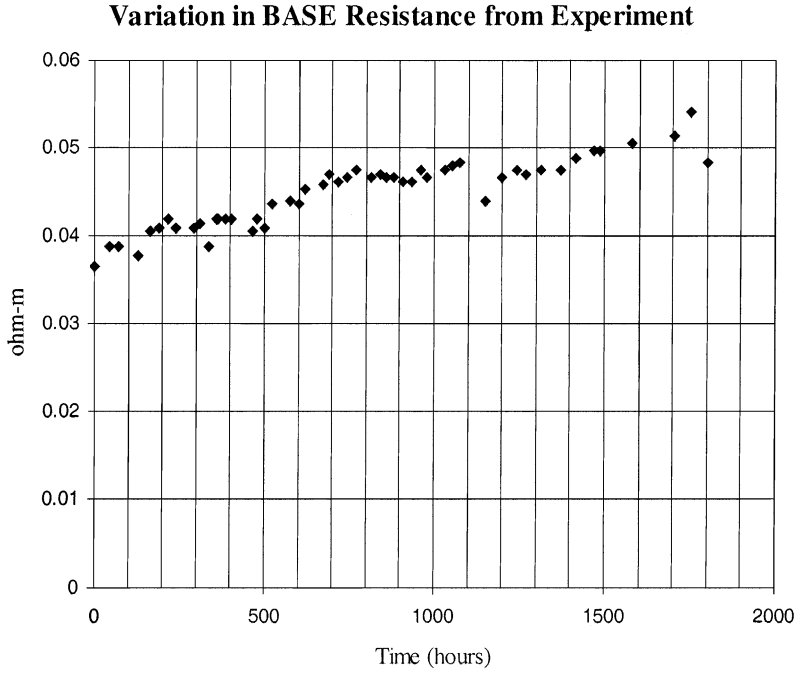

Fig. 4. Experimentally observed variation in BASE resistivity with time.

equations obtained that best described the empirical variation in BASE ionic resistance are given below:

$$\text{Exponential fit}: \quad R_{\text{base}} = 0.71\, e^{(9\times10^{-5}t)} \tag{1}$$

$$\text{Logarithmic fit}: \quad R_{\text{base}} = -1.98 + 0.393 \ln t \tag{2}$$

$$\text{Power fit}: \quad R_{\text{base}} = 0.05 t^{0.374} \tag{3}$$

where R_{base} is the ionic resistance of the BASE and t the time. The regression data for these fits are given in the Appendix A. Of the three, the logarithmic function best fits the BASE resistance variation with the highest correlation coefficient of 0.917. The exponential and power functions also have nearly as high coefficients as this with 0.905 and 0.902, respectively.

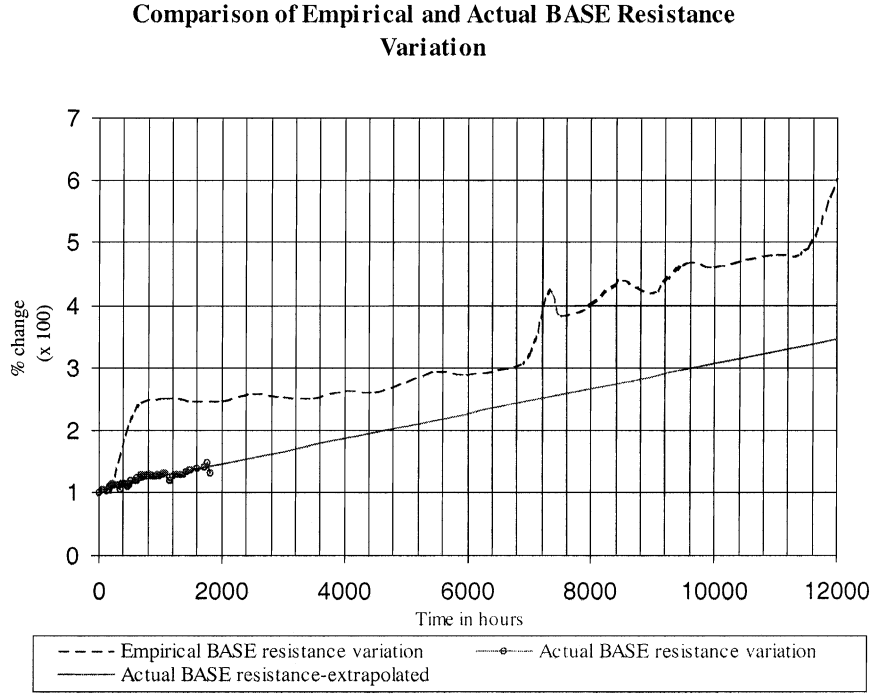

Fig. 5. Comparison of empirical variation in BASE resistance with experimentally observed variation.

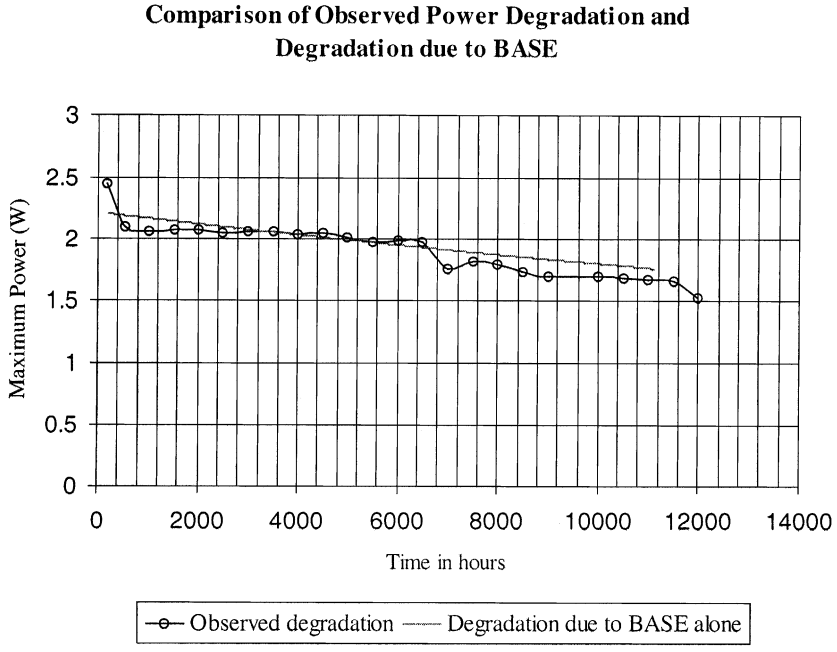

Fig. 6. Comparison of actual power degradation and the degradation caused by the BASE alone.

On using these equations in the simulation code, the power versus time characteristic on the PX-3A that is obtained is similar to the experimentally observed power degradation. It is, therefore, shown that the empirical variation of BASE ionic resistance is a correct model [13].

R.M. Williams et al. conducted experiments on the variation of BASE ionic resistance with time [22]. The β-alumina in the experiments is exposed to a sodium vapor environment with the temperature and pressure conditions similar to those in an AMTEC. As shown in Fig. 4, β-alumina's ionic resistivity shows a gradual increase over 1800 h. This variation in ionic resistance is compared with the empirical variation we obtained in order to determine what proportion of the total variation in the properties of the components of the cell is due to the BASE ionic resistance. Fig. 5 shows a comparison of the empirical BASE resistance variation and the experimentally observed one (extrapolated linearly to 12,000 h) in terms of percentage change. As can be seen, the actual values are less than the empirical. This is only to be expected because the empirical values represent the total internal resistance, which will be higher than BASE resistance alone. The two plots start at almost the same point suggesting that at the start of the operation almost all of the internal resistance is due to the BASE. However, at the end of 12,000 h, the BASE resistance is about 57.8% of the total internal resistance.

The next step is to compare the two power outputs over 100,000 h. One of the outputs is the extrapolated observed power and the other is the time characteristic of the PX-3A empirically obtained from the ionic resistance of the BASE alone. This is done by fitting the experimental data for BASE ionic resistance to a function using regression analysis, and using this function in the APEAM code to obtain time-dependent power output for 100,000 h. The change in BASE ionic resistivity is expressed as percentage change and is fit to a linear function given by the equation of the form

$$y = 0.0002x + 1.0713 \quad (4)$$

where, y represents BASE ionic resistivity, and x time in hours.

It can be seen from Fig. 6 that power degradation due to the BASE alone matches closely with the observed power degradation for up to about 7000 h. Beyond this point, observed degradation is more than that due to the BASE. It can, thus, be concluded that initially (up to 7000 h) the BASE is indeed responsible for practically all of the power degradation. After this point, the effect of changes in the properties of other components begins to contribute to the overall degradation and the separation between the two curves continuously increases with time. Thus, at the end of 100,000 h (see Fig. 7), observed power loss as a percentage of initial value is 92.1% while percentage power loss due to the BASE degradation alone is 75.9% [13,14].

5. Conclusions

It has been established by the results of the analyses that degradation of the BASE is a significant cause of power loss over time. At the end of 12,000 h, for example, the ionic resistance of the BASE is about 58% of the total resistance in

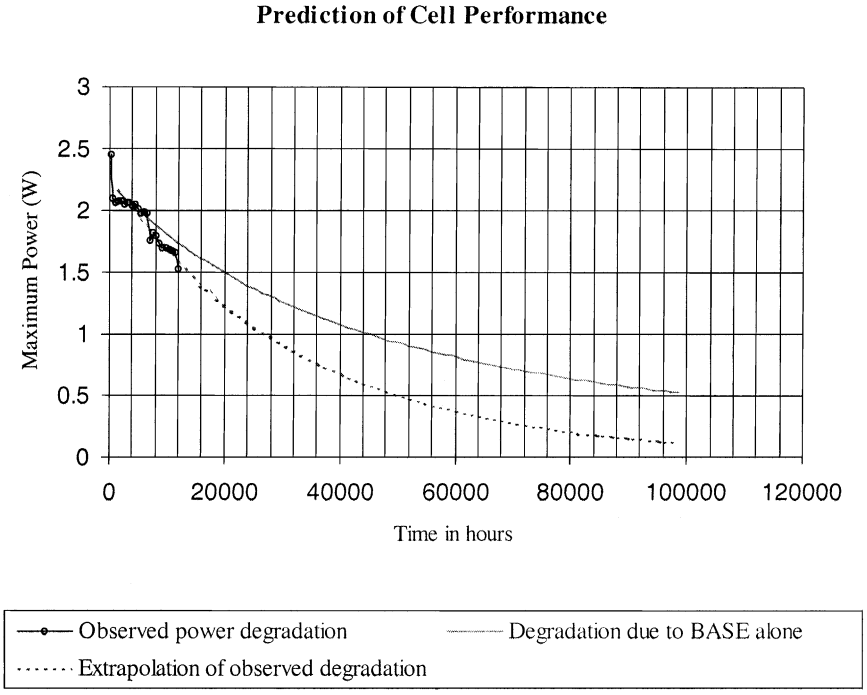

Fig. 7. Extrapolated results of the observed power degradation and that due to the BASE alone.

the cell. For the first 7000 h of cell operation, power loss with time as a result of changes in the ionic resistance of the BASE alone matches very closely with the observed power degradation. After this point, the power versus time curve due to changes in the ionic resistance of the BASE alone and the curve of the observed power degradation begin to diverge continuously. This suggests that after 7000 h, the effect of changes in the other components of the cell begins to adversely influence power output. At the end of 100,000 h, the power output will be about 0.52 W if the effect of BASE ionic resistance alone is taken into account. However, if the observed power degradation maintains its trend for 100,000 h, power output would then be about 0.12 W.

The procedure adopted in this analysis allows the simulation of BASE performance and the effect of changes in the properties of the BASE on power output as a function of time. It also allows the modeling of the observed power degradation (up to 12,000 h) and prediction of this characteristic for up to 100,000 h. Regression analysis is an important tool in this analysis and has been used extensively both to validate some results and for simulation purposes. As a result of this analysis, it is possible to compare to contribution of the BASE to the observed power degradation. The comparison also reveals (as seen by the divergence of the curves in Figs. 5 and 6) that some other components may also be responsible for power degradation. However, the BASE has been shown to be a major cause and the conjecture of this study has been proven correct. These results show that the BASE is responsible to a significant degree for the power degradation.

Appendix A. Regression analysis data of empirical base resistance change with time

Regression data for exponential fit			
Number of observations	26	Regression coefficient (slope)	9.319053e−05
Mean of independent variable	6060.731	Standard error of coefficient	8.898605e−06
Mean of dependent variable	1.169645	*t*-Value for coefficient	10.47249
Standard deviation of independent variable	3597.386	Regression constant (intercept)	0.6048422
Standard deviation of dependent variable	0.37011	Standard error of constant	0.06240194
Correlation coefficient	0.905791	*t*-Value for constant	9.692682

Analysis of variance				
Source	d.f.	Sum of squares	Mean Square	*F*
Regression	1	2.809686	2.809686	109.673
Residual	24	0.6148501	0.02561875	

Regression data for logarithmic fit			
Number of observations	26	Regression coefficient (slope)	0.9174355
Mean of independent variable	8.389204	Standard error of coefficient	0.127622
Mean of dependent variable	3.419231	*t*-Value for coefficient	7.188692
Standard deviation of independent variable	1.027244	Regression constant (intercept)	−4.277322
Standard deviation of dependent variable	1.140465	Standard error of constant	1.078337
Correlation coefficient	0.8263558	*t*-Value for constant	−3.96659

Analysis of variance				
Source	d.f.	Sum of squares	Mean square	*F*
Regression	1	22.20437	22.20437	51.677
Residual	24	10.31217	0.4296736	

Regression data for power fit			
Number of observations	26	Regression coefficient (slope)	0.3250175
Mean of independent variable	8.389204	Standard error of coefficient	0.03173816
Mean of dependent variable	1.169645	*t*-Value for coefficient	10.24059
Standard deviation of independent variable	1.027244	Regression constant (intercept)	−1.556993
Standard deviation of dependent variable	0.37011	Standard error of constant	0.2681704
Correlation coefficient	0.9020894	*t*-Value for constant	−5.805985

Analysis of variance				
Source	d.f.	Sum of squares	Mean square	*F*
Regression	1	2.786768	2.786768	104.8697
Residual	24	0.6377672	0.02657363	

Acknowledgements

We are thankful to John Merrill for providing us the AMTEC operation data prior to publication. This work is supported in part by the United States Air Force Office of Scientific Research via Sub-contract No. F99-0832 CFDA# 12800, Grant No. 98-0001 and the Texas Higher Education Coordinating Board Grant No. ATP 003644-091.

References

[1] G.C. Levy, T.K. Hunt, R.K. Sievers, AMTEC: current status and vision, in: Proceedings of the Intersociety Energy Conversion Engineering Conference, Vol. 2, 1997.
[2] R.K. Sievers, T.K. Hunt, J.F. Ivanenok, M.J. Schuller, Remote condensing for high efficiency AMTEC cells, in: Proceedings of the Intersociety Energy Conversion Engineering Conference, Vol. 1, Conf. 28, 1993.
[3] L. Huang, M.S. El-Genk, M.J. Schuller, Measurements of thermal conductivities of alumina powders and MIN-K in vacuum, in: Proceedings of the Intersociety Energy Conversion Engineering Conference, Vol. 2, 1997.
[4] T. Cole, Thermoelectric energy conversion with solid electrolytes, Science 221 (1983) 4614.
[5] M.A.K. Lodhi, M. Schuller, P. Hausgen, Mathematical modeling for a thermionic-AMTEC cascade system, in: Proceedings of the STAIF'96, American Institute of Physics, pp. 1286–1290.
[6] V.R. Malka, Optimization of the TIEC/AMTEC cascade Cell, Master Thesis, Texas Tech. University, 1998, unpublished.
[7] A. Mustafa, Optimization of AMTEC-TIEC and analysis of the algorithm used for solving the nonlinear system of equations in the thermal model, Master Thesis, Texas Tech. University, 1999, unpublished.
[8] R.M. Williams, M.L. Homer, L. Lara, R.H. Cortez, J. Miller, B. Jeffries-Nakamura, M.L. Underwood, A. Kisor, D. O'Connor, V.B. Shields, K.S. Manatt, M.A. Ryan, Sodium transport modes in AMTEC electrodes, in: Proceedings of the 33rd Intersociety Engineering Conference on Energy Conversion, 2–6 August 1998.
[9] Mark L. Underwood, Roger M. Williams, Margaret A. Ryan, Barbara Jeffries-Nakamura, Dennis O'Connor, An AMTEC vapor–vapor, series connected cell, in: Proceedings of the 9th Symposium on Space Nuclear Power Systems, CONF 920104, 1992, American Institute of Physics, Conference proceedings No. 246, III, pp. 1331–1337.
[10] R.K. Sievers, J.E. Pantolin, R.C. Svedberg, D.A. Butkiewicz, C.A. Borkowski, C. Huang, T.J. Hendricks, T.K. Hunt, Series II AMTEC cell design and development, in: Proceedings of the Intersociety Energy Conversion Engineering Conference, Vol. 2, 1997.
[11] A. Schock, H. Noravian, C. Or, Coupled thermal, electrical, and fluid flow analyses of AMTEC converters, with illustrative application to OSC's cell design, in: Proceedings of the Intersociety Energy Conversion Engineering Conference, Vol. 2, Conf. 32, 1997.
[12] A. Schock, H. Noravian, C. Or, V. Kumar, Design, analysis, and fabrication procedure of AMTEC cell, test assembly, and radio-isotope power system for outer-planet missions, in: Proceedings of the 48th International Astronautical Congress, Turin, Italy, 1997.
[13] P. Vijayaraghavan, Power degradation and performance evaluation of BASE in AMTEC, Master's Thesis, Texas Tech. University, unpublished.
[14] M.A.K. Lodhi, P. Vijayaraghavan, A. Daloglu, Time-dependant BASE performance and power degradation in AMTEC, J. Power Sources 93 (2001) 41–49.
[15] R.M. Williams, M.A. Ryan, M.L. Homer, L. Laura, K. Manatt, V. Shields, R.H. Cortez, J. Kulleck, The thermal decomposition of sodium β-alumina solid electrolyte ceramic in AMTEC cells, Meeting abstracts, Electrochemical Society-all divisions, 1091–8213, No. 1, Electrochemical Society, 1998, p. 831.
[16] J.H. Kennedy, The β-aluminas, Topics in Applied Physics: Solid Electrolytes, Springer, New York, 1977.

[17] M.L. Underwood, R.M. Williams, M.A. Ryan, B. Jeffries-Nakamura, D. O'Connor, An AMTEC vapor–vapor, series connected cell, in: Proceedings of the 9th Symposium on Space Nuclear Power Systems, CONF 920104, American Institute of Physics, Conference Proceedings No. 246, III, 1992, pp. 1331–1337.
[18] J. Tournier, M.S. El-Genk, AMTEC performance and evaluation analysis model: comparison with test results of PX-4C, PX-5A, and PX-3A Cells, in: Proceedings of the 15th Symposium on Space and Nuclear Power and Propulsion, 3rd Space Technology and Applications International Forum, American Institute of Physics, 1998.
[19] V. Ganesan, V. Ganesan, Corrosion of annealed AISI 316 stainless steel in sodium environment, J. Nucl. Mater. 256 (1) (1998) 69.
[20] M.A. Ryan, A. Kisor, R.M. Williams, B. Jeffries-Nakamura, D. O'Connor, Lifetimes of thin film AMTEC electrodes, in: Proceedings of the 29th Intersociety Energy Conversion Engineering Conference.
[21] Donald, L. Alger, Some corrosion failure mechanisms of AMTEC cells, in: Proceedings of the 32nd Intersociety Energy Conversion Engineering Conference, July 1997, J. Intersociety Energy Conversion Eng. Conf. 2 (1997) 1224–1229.
[22] R.M. Williams, M.A. Ryan, M.L. Homer, L. Lara, K. Manatt, V. Shields, R.H. Cortez, J. Kulleck, The thermal stability of sodium β-alumina solid electrolyte ceramic in AMTEC cells, Space Technology and Applications International Forum–1999, The American Institute of Physics, 1999.